

Generalized Multicast Multibeam Precoding for Satellite Communications

Vahid Joroughi, Miguel Ángel Vázquez and Ana I. Pérez-Neira, *Senior Member, IEEE*

Abstract—This paper deals with the problem of precoding in multibeam satellite systems. In contrast to general multiuser multiple-input-multiple-output (MIMO) cellular schemes, multibeam satellite architectures suffer from different challenges. First, satellite communications standards embed more than one user in each frame in order to increase the channel coding gain. This leads to the different so-called multigroup multicast model, whose optimization requires computationally complex operations. Second, when the data traffic is generated by several Earth stations (gateways), the precoding matrix must be distributively computed and meet additional payload restrictions. Third, since the feedback channel is adverse (large delay and quantization errors), the precoding must be able to deal with such uncertainties. In order to solve the aforementioned problems, we propose a two-stage precoding design in order to both limit the multibeam interference and to enhance the intra-beam minimum user signal power (i.e. the one that dictates the rate allocation per beam). A robust version of the proposed precoder based on a first perturbation model is presented. This mechanism behaves well when the channel state information is corrupted. Furthermore, we propose a per beam user grouping mechanism together with its robust version in order to increase the precoding gain. Finally, a method for dealing with the multiple gateway architecture is presented, which offers high throughputs with a low inter-gateway communication. The conceived designs are evaluated with a close-to-real beam pattern and the latest broadband communication standard for satellite communications.

Keywords—Multibeam satellite systems, Precoding, Robust design, Multigroup multicast.

I. INTRODUCTION

A. Motivation

SATELLITE communications will play a central role towards fulfilling next generation 5G communication requirements [1]. As a matter of fact, anytime-anywhere connectivity cannot be conceived without the presence of the satellite segment [2]. Indeed, the satellite industry is not only targeting areas without backbone connectivity (maritime, aeronautic, rural), but also high dense populated scenarios with an existing communication infrastructure, where the satellite

will become an essential element to decongest the terrestrial wireless network.

In order to deliver broadband interactive data traffic, satellite payloads are currently implementing a multibeam radiation pattern. The use of a multibeam architecture brings several advantages in front of a single global beam transmission [3]. First, since an array fed reflector is employed, the antenna gain to noise ratio can be increased leading to high gain of each beam return link achievable throughput. Second, different symbols can be simultaneously sent to geographically separated areas, allowing a spatially multiplexed communication. Last but not least, the available bandwidth can be reused in sufficiently separated beams, leading to an increase of the user bandwidth yet maintaining a low multiuser interference.

Nevertheless, whenever the system designers target the terabit satellite system (i.e. a satellite system offering a terabit per second capacity), the aforementioned multibeam architecture shall be reconsidered. Precisely, full frequency reuse among beams becomes mandatory in order to support the terabit capacity as larger available user bandwidth is required. As a consequence, when considering the satellite forward link, interference mitigation techniques need to be implemented either at the user terminal (multiuser detection) or in the transmitter (precoding).

Whenever precoding is employed, the users must feed back their channel station information (CSI) to the transmitter so that it can revert the interference effect at the transmit side. These techniques rely severely on the quality of the CSI and they dramatically decrease their performance in case CSI is either deprecated or corrupted. On the contrary, multiuser detection techniques does not depend on the feedback channel but; however, the user terminal complexity increases so as its cost. In addition, precoding system level studies are providing encouraging results for implementing this technique in real multibeam satellite systems [4]. As a result, we will consider precoding as the interference reliever for the present study.

B. Previous Works

The first designs of precoding techniques for multibeam satellite systems can be found in [5]. Mimicking the linear techniques for multiuser multiple-input-multiple-output (MIMO) schemes the authors propose a zero forcing (ZF) and minimum mean square error (MMSE) precoding designs. In addition, several challenges for the implementation of precoding in multibeam satellite systems were pointed out. We describe them in the following.

As a general statement, the payload complexity shall be maintained low and; consequently, the ground segment must

The research leading to these results has received funding from the Spanish Ministry of Science and Innovation under projects TEC2014-59225-C3-1-R (ELISA) and the Catalan Government (2014 SGR 1567).

V. Joroughi is with the Universidad de Vigo, Pontevedra, Vigo, Spain.

Email: vahid.joroughi@gti.uvigo.es

A. Pérez-Neira is with the Universitat Politècnica de Catalunya (UPC) and Centre Tecnològic de les Telecomunicacions de Catalunya (CTTC), Barcelona, Spain.

Email: ana.isabel.perez@upc.edu

M. Á. Vázquez is with the CTTC, Barcelona, Spain.

Email: mavazquez@cttc.es

perform most of the computations and transmit the precoded signals through the feeder link. This feeder link must be able to support the overall satellite traffic, leading to a very large bandwidth requirement. This requirement is even larger when precoding is deployed at the gateway since the feed signals must be precoded and simultaneously transmitted through the feeder link. On the other hand, if the payload is equipped with a beamforming mechanism, the feeder link bandwidth requirements can be alleviated since only the user signals shall be transmitted¹. However, as presented in [6], [7] on board processing limits the overall gains obtained by the on ground processing [8], [9]. Remarkably, in case the on board processing is optimized considering an underlying precoding scheme, certain throughput gain can be preserved [10]. Yet another alternative is to shift the feeder link to the Q/V bands although certain diversity schemes must be deployed for dealing with the large path loss [11].

In order to deal with the increasing requirement of feeder link bandwidth that results from the full frequency beam reuse pattern, several Earth stations (gateways) can be deployed. With this, the available spectrum for the feeder link can be reused among spatially separated gateways through very directive antennas. In these systems, the traffic is generated at different gateways so that several feeder links simultaneously transmit precoded data from isolated areas. As a consequence, the precoding technique shall be reconsidered since, in order to have enough spectrum to access all the feeds, each gateway has only access to a certain set of feeds. In [12], [13] a precoding scheme based on the regularized ZF scheme is presented. As a matter of fact, the overall throughput is reduced when multiple gateways are considered even though computationally complex on ground schemes are deployed [14].

Last, but not least, satellite communications operate in a multicast fashion since data from different users is embedded in the same frame. Precisely, in order to increase the coding gain, each beam simultaneously serves more than one user by means of transmitting a single coded frame. This scheme entails a modification of the overall precoding scheme since more than one spatial signature per beam must be considered and; moreover, the achievable rate is dictated by the user with the lowest signal-to-noise-plus-interference ratio (SNIR). The first approach for solving this problem can be found in [15] where a sequential beamforming scheme is presented. However, whenever a large number of beams over the coverage area is targeted, one-shot scheme must be implemented. An example of this can be found in [16] where a design based on MMSE precoding and channel averaging is presented. Since the multicast multibeam transmission can be cast as multigroup multicast mathematical model, the proposed designs in [17] can be applied. Finally, very high throughputs can be obtained whenever the joint precoding and user scheduling is performed as in [18].

¹This statement assumes that the number of feeds is larger than the number of users as it happens in most of the current deployments. This will be discussed in Section II.

C. Contributions

In contrast to the aforementioned works, the present paper proposes a low complex ground precoding scheme to deal with the multibeam interference in multicast transmissions. The presented novel technique is based on two stage linear precoding similar to [19], where the multiuser MIMO scenario is targeted. Our proposal offers higher spectral efficiencies than the regularized ZF [17], the average MMSE scheme [16] and the frame-based precoding scheme [18] yet maintaining a low computational complexity. It is important to remark that we prioritize low complex one-shot design in front of iterative interior point methods such as [14].

In addition, considering that the CSI will be corrupted at the gateway, a robust scheme is presented based on the first order perturbation theory of the eigenvectors and eigenvalues [20]. This robust design is novel and it offers sufficiently large throughputs even if the CSI is corrupted. The resulting precoding design remains low complex so that it can be implemented even if a very large number of feeds are considered. Remarkably, this differs from the aforementioned work where the general CSI uncertainty is not tackled.

Since the achievable rates decrease whenever the user channel vectors within one beam are not collinear, we propose a user grouping technique. With this, over all possible users to be served for each beam, we select the most adequate ones using a variation of the k -means algorithm. This algorithm differs from the one presented in [16] as not only the channel magnitudes but the phase effects are considered. Moreover, the proposed approach differs to the one presented in [18] where a joint scheduling precoding optimization is presented. Additionally, a novel robust user grouping scheme is proposed in order to deal with the possible channel uncertainties.

In case the data traffic is generated by several gateways, a precoding mechanism is presented for dealing with the main challenges; namely, CSI sharing and the distributed precoding matrix computation. Both a reduced inter-gateway communication for CSI sharing and a precoding matrix division among gateways are presented. Even though the achievable rates are decreased when the multiple gateway architecture is considered, the proposed scheme offers a good trade-off between communication overhead, payload complexity and overall throughput.

The rest of the paper is organized as follows. Section II introduces the problem so as the channel modelling. Based on this model and problem statement, Section III presents the two stage precoding design for dealing with both the multibeam interference and intra-beam signal enhancement. Relying on a certain precoding design, a robust scheme is proposed based on the first order perturbation method in Section IV. Section V shows how to implement precoding in a multiple gateway architecture. Section VI presents numerical simulations considering the digital video broadband S2X (DVB-S2X) and a beam pattern of 245 beams. Section VII concludes.

Notation: We adopt the notation of using lower case boldface for vectors, \mathbf{v} , and upper case boldface for matrices, \mathbf{A} . The transpose operator and the conjugate transpose operator are denoted by the symbols $(\cdot)^T$, $(\cdot)^H$ respectively. $\mathbf{E}[\cdot]$ de-

notes expectation. \mathbf{I} denotes the identity matrix. \mathbb{C} denotes the complex numbers. $\|\cdot\|$ denotes the Euclidean norm. $|\cdot|$ denotes the absolute value. \preceq denotes the componentwise inequality. \circ denotes the Hadamard product. $\mathcal{O}(f(n))$ denotes asymptotic upper bound computational complexity over n .

II. PROBLEM FORMULATION

A. Channel Model

Let us consider a multibeam broadband satellite with fixed receivers where a single gateway is provisioning signals to be transmitted through a feeder link. Over the feeder link², a total number of N feed signals are frequency multiplexed so that the payload has to detect and route them through an array fed reflector. This array fed reflector transforms the N feed signals into K transmitted signals (i.e. one signal per beam) to be radiated over the multibeam coverage area.

As a matter of fact, the array fed reflector can have a single-feed-per-beam (SFPB) architecture whenever $N = K$ or a multiple-feed-per-beam (MFPB) when $N > K$. This latter payload architecture presents lower beamforming scan losses and larger antenna gains than the SFPB [21]. For the sake of generality we will consider the MFPB structure in the rest of the paper.

It is important to remark that this satellite transmission scheme is coined as on ground beamforming. This technique has been widely used for mobile satellite services by means of deploying satellites such as Terrestar-1, ICO-G1 or Skyterra-1. In addition, it is worth mentioning that the N feed signals could allocate signals for different polarizations.

Towards a spectrally efficient communication, all beams share the frequency band and; in a given time instant, the k -th beam simultaneously serves a total amount of Q_k users. In other words, in a give time instant the scheduler selects a set of Q_k users at the k -th beam (same for all beams) and it constructs a codeword with information to be transmitted to all Q_k . Without loss of generally, we will assume that each beam serves the same number of users simultaneously and it is equal to Q (i.e. $Q_k = Q \quad k = 1, \dots, K$). Figure 1 shows the overall system.

Under this context, the received signal can be modelled as

$$\mathbf{y} = \mathbf{H}\mathbf{x} + \mathbf{n} \quad (1)$$

where $\mathbf{y} \in \mathbb{C}^{KQ \times 1}$ is a vector containing the received signals at each user terminal. Vector $\mathbf{n} \in \mathbb{C}^{KQ \times 1}$ contains the noise terms of each user terminal and we will assume that they are Gaussian distributed with zero mean, unit variance and uncorrelated with both the desired signal and the other users noise terms (i.e. $E[\mathbf{n}\mathbf{n}^H] = \mathbf{I}_{KQ}$).

We assume independent channel realizations in different time instants. The channel matrix can be described as follows

$$\mathbf{H} = \mathbf{F} \circ \Phi. \quad (2)$$

Matrix $\mathbf{F} \in \mathbb{R}^{KQ \times N}$ represents signal attenuation generated via both the atmospheric fading and the antenna feed radiation.

²The feeder link connection is considered ideal. This is, noiseless and without channel impairments.

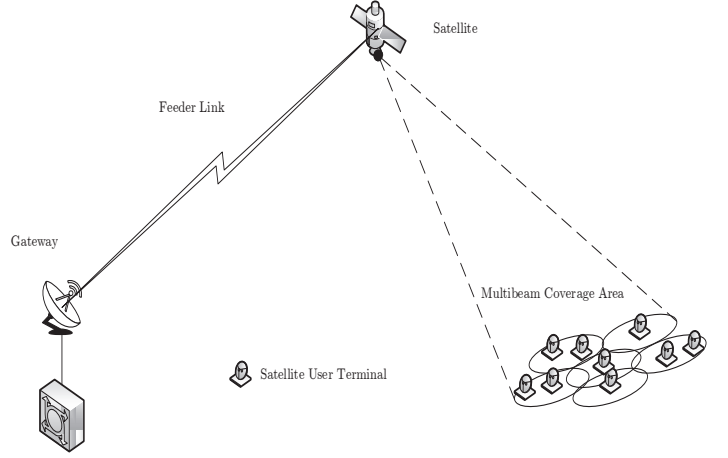


Fig. 1. The picture depicts the multicast multibeam satellite structure. The gateway delivers certain data to the coverage area by first the feeder link and; posteriorly, the satellite. While the feeder link multiplexes N signals, the satellite that is equipped with an array fed reflector, radiated a total of K signals (one signal per beam). Every radiated signal by the satellite shall be detected by a total number of Q users per beam.

This matrix can be decomposed as follows

$$\mathbf{F} = \mathbf{A}\mathbf{G} \quad (3)$$

where $\mathbf{A} \in \mathbb{R}^{KQ \times KQ}$ is diagonal matrix whose diagonal entries are the atmospheric fading terms corresponding to the q -th user in the k -th beam. Matrix $\mathbf{G} \in \mathbb{R}^{KQ \times N}$ takes into account the rest of gain and loss factors. Its (kq, n) -th entry can be described as follows

$$[G]_{k,n} = \frac{G_R a_{kqn}}{4\pi \frac{d_{kq}}{\lambda} \sqrt{K_B T_R B_W}} \quad (4)$$

with d_{kqn} the distance between the q -th user terminal in the k -th beam and the satellite. λ is the carrier wavelength, K_B is the Boltzmann constant, B_W is the carrier bandwidth, G_R^2 the user terminal receive antenna gain, and T_R the receiver noise temperature. The term a_{kqn} refers to the gain from the n -th feed to the q -th user in the k -th beam. It is important to mention that the \mathbf{G} matrix has been normalized to the receiver noise term.

Furthermore, matrix $\Phi \in \mathbb{C}^{KQ \times N}$ represents the phase variation effects between the n -th feed signal and the q -th user located in the k -th beam. Each entry is defined as

$$[\Phi]_{q,n} = e^{j\theta_{q,n}} \quad (5)$$

where $\theta_{q,n}$ is uniformly distributed between 0 and 2π .

The aforementioned phase effect determines the performance of the system severely. Due to that, an option is to use ultra stable oscillators so that the phase variation due to the different feed oscillators is reduced. With this, we can assume another phase distribution such that

$$\theta_{q,n}^{ultra} = \phi_q + \gamma_{q,n} \quad (6)$$

where ϕ_q is a uniformly distributed in 0 and 2π and $\gamma_{q,n}$ is modelled as a zero mean Gaussian distribution with variance χ^2 . This phase random distribution takes into account that the phase offsets due to the radio-frequency signal propagation path, approximately constant across all the antenna feeds radiating the signal to one receiver (i.e. ϕ_q takes the same value over all feeds n). Moreover, it is considered that the payload oscillator phase offsets have a Gaussian distribution with zero mean and variance of $\chi_{\text{osc}}^2 = 20$ degrees for standard space-qualified devices, or $\chi_{\text{ultra-osc}}^2 = 2$ degrees with ultra-stable oscillators. This phase distribution model is first presented in [16] in the context of an European Space Agency project [22].

For notation convenience, it is better to define $\mathbf{H}_k \in \mathbb{C}^{Q \times N}$ as the channel matrix for the k -th beam so that

$$\mathbf{H} = [\mathbf{H}_1^T, \mathbf{H}_2^T, \dots, \mathbf{H}_K^T]^T. \quad (7)$$

Moreover, the channel vector of the q -th user in the k -th beam is defined as $\mathbf{h}_{k,q}$ so that

$$\mathbf{H}_k = [\mathbf{h}_{k,1}^T, \mathbf{h}_{k,2}^T, \dots, \mathbf{h}_{k,Q}^T]^T. \quad (8)$$

In order to minimize the multiuser interference resulting from the full frequency reuse, linear precoding is considered. Under this context, the transmitted symbol can be modelled as

$$\mathbf{x} = \mathbf{W}\mathbf{s} \quad (9)$$

where $\mathbf{s} \in \mathbb{C}^{K \times 1}$ is a vector that contains the transmitted symbols which we assume uncorrelated and unit norm ($E[\mathbf{s}\mathbf{s}^H] = \mathbf{I}_K$). Matrix $\mathbf{W} \in \mathbb{C}^{N \times K}$ is the linear precoding matrix to be designed.

B. Precoding Design

Let us formulate the precoding design of a multicast multi-beam satellite system. The overall system performance can be optimized considering the maximum sum rate:

$$\begin{aligned} & \underset{\mathbf{W}}{\text{maximize}} \quad \sum_{k=1}^K \text{minimum}_{q=1, \dots, Q} r_{k,q} \\ & \text{subject to} \\ & \text{Tr}(\mathbf{W}\mathbf{W}^H) \leq P_T \end{aligned} \quad (10)$$

where $r_{q,k}$ denotes the achievable rate of the q -th user at the k -th beam,

$$r_{k,q} = \log_2(1 + \text{SINR}_{k,q}), \quad (11)$$

P_T denotes the available power at the satellite, \mathbf{w}_k corresponds to the k -th column of matrix \mathbf{W} and

$$\text{SINR}_{k,q} = \frac{|\mathbf{h}_{q,k}^H \mathbf{w}_k|^2}{\sum_{j \neq k} |\mathbf{h}_{q,k}^H \mathbf{w}_j|^2 + 1}. \quad (12)$$

It is important to remark that even though power sharing mechanisms among beams can be implemented [23], [24] their deployment into next generation satellite payloads will require costly and complex radio-frequency designs. Under this context, the precoding design shall consider a per-feed available power constraint so that the constraint in (10) becomes

$$(\mathbf{W}\mathbf{W}^H)_{n,n} \leq \frac{P_T}{N} \quad n = 1, \dots, N, \quad (13)$$

where it has been assumed that the available power is equally share by all feed elements.

In any case, problem (10) is a difficult non-convex problem whose convex relaxations even require computationally demanding operations [25]. For multibeam satellite systems the computational complexity of the precoding design is an essential feature since these systems usually operate with hundreds of beams. Consequently, in contrast to other works, the target of this paper is to design a low computationally complex precoding scheme able to achieve high throughput values.

In the next section we propose a precoding technique that splits the precoding matrix in an interference mitigation precoder and an intra-frame rate maximization matrix. Remarkably, there is no theoretical background to support that by doing this one can attain a higher throughput than in a sum-rate maximizing algorithm like in [18]. Still, as it is described in the following sections, large data rates similar to the ones of the sum rate maximization are obtained in the numerical evaluations while preserving a very low complexity.

III. GENERALIZED MULTICAST MULTIBEAM PRECODING

The precoding design in multicast multibeam satellite systems has to main roles. First, the inter-beam interference shall be minimized and; second, the precoding shall increase the lowest SINR within each beam. Under this context, the precoding design can be divided into two sub-matrices such as

$$\mathbf{W} = \alpha \mathbf{W}_a \mathbf{W}_b, \quad (14)$$

where

$$\mathbf{W}_a = [\mathbf{W}_{a_1}, \dots, \mathbf{W}_{a_K}] \in \mathbb{C}^{N \times KQ}, \quad (15)$$

and

$$\mathbf{W}_b = \begin{bmatrix} \mathbf{w}_{b_1} & \mathbf{0} & \dots & \mathbf{0} \\ \mathbf{0} & \mathbf{w}_{b_2} & \dots & \mathbf{0} \\ \vdots & \vdots & \ddots & \vdots \\ \mathbf{0} & \mathbf{0} & \dots & \mathbf{w}_{b_K} \end{bmatrix} \in \mathbb{C}^{KQ \times K}, \quad (16)$$

with $\mathbf{W}_{a_k} \in \mathbb{C}^{N \times Q}$ and $\mathbf{w}_{b_k} \in \mathbb{C}^{Q \times 1}$. The matrix \mathbf{W}_a is used to mitigate the inter-beam interference first and then the matrix \mathbf{W}_b is used to optimize the intra-frame data rate (i.e. the rate of the served users) so that \mathbf{w}_{b_k} and \mathbf{W}_{a_k} denotes the precoding for optimizing the rate at k -th beam. Finally, the parameter α is chosen to set the available power constraint (both for the per feed and total power constraint).

In the following subsections, two different designs for \mathbf{W}_a and a single design for \mathbf{W}_b are presented.

A. Inter-beam Interference Mitigation Precoding

1) *Multibeam Interference Mitigation (MBIM)*: Let us define $\tilde{\mathbf{H}}_k$ as

$$\tilde{\mathbf{H}}_k = \begin{bmatrix} \mathbf{H}_1 \\ \vdots \\ \mathbf{H}_{k-1} \\ \mathbf{H}_{k+1} \\ \vdots \\ \mathbf{H}_K \end{bmatrix} \in \mathbb{C}^{(K-1)Q \times N}. \quad (17)$$

First we observe the interference impact of the precoding matrix \mathbf{W}_a . This can be done by means of constructing the equivalent combined channel matrix after the precoding effect:

$$\mathbf{H}\mathbf{W}_a = \begin{bmatrix} \mathbf{H}_1\mathbf{W}_{a_1} & \mathbf{H}_1\mathbf{W}_{a_2} & \cdots & \mathbf{H}_1\mathbf{W}_{a_K} \\ \mathbf{H}_2\mathbf{W}_{a_1} & \mathbf{H}_2\mathbf{W}_{a_2} & \cdots & \mathbf{H}_2\mathbf{W}_{a_K} \\ \vdots & \vdots & \ddots & \vdots \\ \mathbf{H}_K\mathbf{W}_{a_1} & \mathbf{H}_K\mathbf{W}_{a_2} & \cdots & \mathbf{H}_K\mathbf{W}_{a_K} \end{bmatrix}, \quad (18)$$

where the k -th beam effective channel is given by $\mathbf{H}_k\mathbf{W}_{a_k}$ and the interference generated to the other users is determined by $\tilde{\mathbf{H}}_k\mathbf{W}_{a_k}$.

As described in [19] an efficient design of \mathbf{W}_a is given by the optimal matrix of the following modified MMSE objective function

$$\underset{\mathbf{W}_a}{\text{minimize}} \quad \mathbb{E} \left[\sum_{k=1}^K \|\tilde{\mathbf{H}}_k\mathbf{W}_{a_k}\|^2 + \frac{KQ}{P_T} \|\mathbf{n}\|^2 \right]. \quad (19)$$

where the term $\frac{KQ}{P_T}$ is obtained considering a total power constraint.

The solution of this optimization problem is given by

$$\mathbf{W}_{a_k}^{\text{MBIM}} = \mathbf{M}_{a_k} \mathbf{D}_{a_k}, \quad (20)$$

where

$$\mathbf{M}_{a_k} = \tilde{\mathbf{V}}_k, \quad (21)$$

and

$$\mathbf{D}_{a_k} = \left(\tilde{\mathbf{\Sigma}}_k + \frac{KQ}{P_T} \mathbf{I} \right)^{-1/2}. \quad (22)$$

Note that it has been considered the singular value decomposition of $\tilde{\mathbf{H}}_k^H \tilde{\mathbf{H}}_k = \tilde{\mathbf{V}}_k \tilde{\mathbf{\Sigma}}_k \tilde{\mathbf{V}}_k^H$.

2) *Regularized Zero-Forcing*: Let $\mathbf{H}^{(R)} \in \mathbb{C}^{KQ \times KQ}$ denote the regularized channel defined as

$$\mathbf{H}^{(R)} = \mathbf{H}\mathbf{H}^H + \frac{KQ}{P_T} \mathbf{I}, \quad (23)$$

where the same regularization factor as that of the multicast-aware regularized zero-forcing [17] is considered. Let us define

$\tilde{\mathbf{H}}_k^{(R)}$ as

$$\tilde{\mathbf{H}}_k^{(R)} = \begin{bmatrix} \tilde{\mathbf{H}}_1^{(R)} \\ \vdots \\ \tilde{\mathbf{H}}_{k-1}^{(R)} \\ \tilde{\mathbf{H}}_{k+1}^{(R)} \\ \vdots \\ \tilde{\mathbf{H}}_K^{(R)} \end{bmatrix} \in \mathbb{C}^{K(Q-1) \times KQ}. \quad (24)$$

The SVD decomposition of matrix can be described as

$$\tilde{\mathbf{H}}_k^{(R)} = \tilde{\mathbf{U}}_k^{(R)} \tilde{\mathbf{\Sigma}}_k^{(R)} \begin{bmatrix} \tilde{\mathbf{V}}_k^{(R),1} & \tilde{\mathbf{V}}_k^{(R),0} \end{bmatrix}^H, \quad (25)$$

where it is emphasized that there is always a null space of dimension Q spanned by $\tilde{\mathbf{V}}_k^{(R),0}$. This matrix is used for this scheme such as

$$\mathbf{W}_{a_k}^{\text{R-ZF}} = \mathbf{H}^H \tilde{\mathbf{V}}_k^{(R),0} \in \mathbb{C}^{N \times Q}. \quad (26)$$

B. Intra-beam Precoding

After the first precoding scheme, \mathbf{W}_a , the k -th beam observes an equivalent channel $\mathbf{Z}_k = \mathbf{H}_k\mathbf{W}_{a_k} \in \mathbb{C}^{Q \times N}$. Based on \mathbf{Z}_k the system designer shall construct \mathbf{w}_{b_k} . Let us mention that the equivalent channel for the q -th user located at the k -th beam is denoted by $\mathbf{z}_{k_q} \in \mathbb{C}^{N \times 1}$ so that

$$\mathbf{Z}_k = [\mathbf{z}_{k_1}, \dots, \mathbf{z}_{k_Q}]. \quad (27)$$

A suboptimal yet efficient approach is to maximize the average SNR considering the equivalent channel matrix. This is done with the following optimization problem

$$\begin{aligned} & \underset{\mathbf{w}_{b_k}}{\text{maximize}} \quad \sum_{q=1}^Q |\mathbf{z}_{k_q}^H \mathbf{w}_{b_k}|^2 \\ & \text{subject to} \quad \|\mathbf{w}_{b_k}\|^2 \leq 1. \end{aligned} \quad (28)$$

Since the objective function in (28) can be re-written as $\|\mathbf{Z}_k \mathbf{w}_{b_k}\|^2$, the optimal solution of (28) is given by the eigenvector associated to the largest eigenvalue of matrix \mathbf{Z}_k . Note that this precoding design offers a low computational complexity since only the eigenvector associated to the largest eigenvalue needs to be computed.

C. Power control

Once both precoding schemes are computed, it is time to calculate the value of α in order to fulfil the maximum transmit power constraints. In case the maximum per feed available power constraint is considered,

$$\alpha = \frac{P_T}{N \max_i \left((\mathbf{W}\mathbf{W}^H)_{i,i} \right)}, \quad (29)$$

whereas in case total power constraints are considered

$$\alpha = \frac{P_T}{N \text{Tr} \left((\mathbf{W}\mathbf{W}^H)_{i,i} \right)}. \quad (30)$$

D. Computational Complexity

This subsection aims at describing the computational complexity of the proposed precoding methods. The aforementioned methods can be described as three main consecutive computations namely; inter-beam precoding, intra-beam precoding and power control. Let us describe the computational complexity of each sub-part. Remarkably, the matrix multiplications operations have not been considered as its computational complexity ($\mathcal{O}(NMP)$ for $N \times M$ matrix multiplied by a $M \times P$ matrix) is lower than the remaining operations.

The intra-beam precoding computational complexity is dictated by the computation of a set of K SVD decompositions. As a matter of fact computing the SVD decomposition of $M \times N$ is $\mathcal{O}(aM^2N + bN^3)$ where a and b are constant values which depend on the method used [26]. Under this context, the MBIM technique intra-beam precoding has a computational complexity of

$$\mathcal{O}\left(K\left(a((K-1)Q)^2N + bN^3\right)\right), \quad (31)$$

whereas the regularized zero forcing one

$$\mathcal{O}\left(K\left(a((Q-1)K)^2KQ + b(KQ)^3\right)\right). \quad (32)$$

On the other hand, intra-beam precoding computational complexity is dictated by an eigenvector decomposition of $N \times N$ matrix which has a computational complexity of $\mathcal{O}(N^3)$. Finally, the power allocation scheme either requires the sum of N values or finding the maximum of N values which in both cases the computational complexity is $\mathcal{O}(N)$.

By the asymptotic composition rule of computational complexity [27], the resulting computational complexity for both schemes are

$$\mathcal{C}_{\text{MBIM}} = \mathcal{O}(K^3Q^2N) \quad (33)$$

$$\mathcal{C}_{\text{RZF}} = \mathcal{O}(K^4Q^3). \quad (34)$$

The aforementioned computational complexities differ from the method reported in [18] as we show in the following.

The multigroup multicast sum-rate optimization with per antenna power method recursively employs two iterative methods in which each of them a relaxed semidefinite program and a least square method are solved respectively. In the first iterative method the computational complexity becomes $\mathcal{O}(N^{10})$ since at least N iterations with a complexity of $\mathcal{O}(N^9)$ are required as reported in [18]. Moreover, for each semidefinite relaxation solution, a randomization jointly with a linear program optimization shall be carried out. As a result, the computational complexity for this sub-iteration becomes

$$\mathcal{O}(N^{13.5}N_{\text{rand}}\log(1/\epsilon)), \quad (35)$$

where N_{rand} the number of randomizations required by the semidefinite relaxation technique and it has been considered that the linear program optimization leading to an accuracy of ϵ requires a computational complexity of $\mathcal{O}(N^{3.5}\log(1/\epsilon))$.

The second iterative process consists of a subgradient constant calculation and a least square with equality constraints. Both schemes have lower computational complexity

that the previously reported so that they can be neglected. Bearing this in mind, the computational complexity of the sum-rate multigroup multicast method with per antenna power constraints becomes

$$\mathcal{C}_{\text{PAC}} = \mathcal{O}(N_{\text{itera}}N^{13.5}N_{\text{rand}}\log(1/\epsilon)), \quad (36)$$

where N_{itera} is the number of required iterations. As it can be observed, our proposed methods show a lower asymptotic computational complexity than the one reported in [18]. Remarkably, in order to determine the best algorithm election for a final hardware implementation will require a deeper analysis than the one presented in this subsection. Indeed, the final computational resources to be used strongly depend on the tentative hardware optimization and the computation details. This analysis is out of the scope of this paper which only states the asymptotic computational complexity of both the schemes.

IV. ROBUST MULTICAST MULTIBEAM PRECODING

As it will be shown in the simulation section, the MBIM schemes offers larger achievable rates than the R-ZF. Consequently, we will consider this design so as the average optimization intra-beam method. In any case, note that precoding performance relies on an accurate CSI fed back by the receiver. However, this CSI suffers from certain degradation due to quantization and transmission delay. Due to that, it is convenient to reformulate the optimization problem in order to take into account these possible variations [28]. This is done in the following subsections for both the inter-beam and intra-beam precoding.

First, let us introduce the perturbation where the transmitter do not longer have access to \mathbf{H} but to a degraded version such as

$$\hat{\mathbf{H}} = \mathbf{H} + \mathbf{\Delta}, \quad (37)$$

where $\mathbf{\Delta} \in \mathbb{C}^{K \times N}$ is the perturbation matrix where it is assumed to be constrained so that

$$\|\mathbf{\Delta}\|^2 \leq \gamma. \quad (38)$$

For notational convenience, it is important to define the following sub-matrices

$$\mathbf{\Delta} = [\mathbf{\Delta}_1^T, \mathbf{\Delta}_2^T, \dots, \mathbf{\Delta}_K^T]^T, \quad (39)$$

$$\mathbf{\Delta}_k = [\delta_{k,1}^T, \delta_{k,2}^T, \dots, \delta_{k,Q}^T]^T, \quad (40)$$

$$\tilde{\mathbf{\Delta}}_k = \begin{bmatrix} \mathbf{\Delta}_1 \\ \vdots \\ \mathbf{\Delta}_{k-1} \\ \mathbf{\Delta}_{k+1} \\ \vdots \\ \mathbf{\Delta}_K \end{bmatrix} \in \mathbb{C}^{(K-1)Q \times N}, \quad (41)$$

where $\mathbf{\Delta}_k \in \mathbb{C}^{Q \times N}$ is the perturbation associated to the k -th beam, $\delta_{k,q} \in \mathbb{C}^{N \times 1}$ is the perturbation associated to the

q -th user located at the k -th beam. Under this context, the perturbation sub-matrices can be constrained as follows

$$\|\Delta_k\|^2 \leq \gamma_k, \quad (42)$$

$$\|\tilde{\Delta}_k\|^2 \leq \tilde{\gamma}_k, \quad (43)$$

for $k = 1 \dots, K$ and where

$$\tilde{\gamma}_k = \sum_{l \neq k}^K \gamma_l. \quad (44)$$

Additionally, a definition of a lower bound of the perturbation matrices Δ_k is convenient

$$\|\Delta_k\|^2 \geq \underline{\gamma}_k. \quad (45)$$

Remarkably, finding the adequate γ bounds for all different perturbation matrices is not an easy task. Indeed, the computation of the different bounds shall be done on an empirical basis considering the different error sources and their final value on the perturbation matrix. This study is out of the scope of this paper and we will only provide a sensitivity analysis in the simulation section.

A. Robust Inter-beam Precoding

Considering the MBIM scheme presented in the previous section, whenever the robust worst-case optimization problem (19) is targeted, the following new optimization problem shall be considered

$$\begin{aligned} & \underset{\mathbf{W}_a}{\text{minimize}} \quad \underset{\{\tilde{\Delta}_k\}_{k=1}^K}{\text{maximize}} \quad \mathbb{E} \left[\sum_{k=1}^K \|\hat{\mathbf{H}}_k \mathbf{W}_{a_k}\|^2 + \frac{KQ}{P_T} \|\mathbf{n}\|^2 \right] \\ & \text{subject to} \\ & \|\tilde{\Delta}_k\|^2 \leq \tilde{\gamma}_k \quad k = 1, \dots, K, \end{aligned} \quad (46)$$

where $\hat{\mathbf{H}}_k = \tilde{\mathbf{H}}_k + \tilde{\Delta}_k$. Considering that the optimal design on (19) leads to the computation of an eigendecomposition, the perturbation matrix will both impact the eigenvectors and eigenvalues. Robust designs generally only consider the effect on the eigenvalues [29, Chapter 7]; however, the impact on the eigenvectors cannot be considered negligible [20].

The following theorem provides an approximate solution of the optimization problem in (46).

Theorem 1 *The optimal inter-beam precoding matrix which approximately minimizes (46) is*

$$\widehat{\mathbf{W}}_{a_k}^{MBIM} = \widehat{\mathbf{M}}_{a_k} \widehat{\mathbf{D}}_{a_k}, \quad (47)$$

where

$$\widehat{\mathbf{M}}_{a_k} = \tilde{\mathbf{V}}_k \left(\tilde{\mathbf{R}}_k + \mathbf{I} \right) \quad (48)$$

and

$$\widehat{\mathbf{D}}_{a_k} = \left(\tilde{\Sigma}_k + \epsilon_k \mathbf{I} \right)^{-1/2} \quad (49)$$

where

$$\epsilon_k = \hat{\gamma}_k^2 + 2\hat{\gamma}_k \sigma_{\max} \left(\tilde{\mathbf{H}}_k^H \tilde{\mathbf{H}}_k \right). \quad (50)$$

The rest of the matrices are defined in Appendix A and not included here for the sake of brevity.

Proof: See Appendix A. ■

Remarkably, whenever ϵ_k increases, the resulting robust precoding design is more different than the original design $\mathbf{W}_{a_k}^{\text{MMSE}}$. In any case, the computational complexity of the robust design remains the same.

B. Robust Intra-beam Precoding

Similarly to the previous robust design the intra-beam precoding shall consider tentative perturbations on their channel matrices. Considering the average optimization scheme, worst-case robust optimization for the k -th beam can be described as the following optimization problem

$$\begin{aligned} & \underset{\mathbf{w}_{b_k}}{\text{maximize}} \quad \underset{\Delta_k}{\text{minimize}} \quad \|\hat{\mathbf{Z}}_k \mathbf{w}_{b_k}\|^2 \\ & \text{subject to} \\ & \|\mathbf{w}_{b_k}\|^2 = 1, \\ & \|\Delta_k\|^2 \geq \underline{\gamma}_k, \end{aligned} \quad (51)$$

where

$$\hat{\mathbf{Z}}_k = \mathbf{H}_k \mathbf{W}_{a_k} + \Delta_k \mathbf{W}_{a_k}. \quad (52)$$

The next theorem presents an approximate solution of the aforementioned problem.

Theorem 2 *An approximate solution of (51) is $\hat{\mathbf{z}}_{k1}$, which is the first column vector of matrix*

$$\mathbf{L}_k \left(\nu_k \mathbf{N} \circ \left(\mathbf{L}_k^H \mathbf{L}_k^H \mathbf{T}_k + \mathbf{T}_k \mathbf{L}_k^H \mathbf{L}_k \right) + \mathbf{I} \right) \quad (53)$$

where

$$\nu_k = \underline{\gamma}_k \mathbf{1}^T \left(\tilde{\Sigma}_k + \epsilon_k \mathbf{I} \right)^{-1/2} \mathbf{1}, \quad (54)$$

and the rest of matrices are defined in Appendix B.

Proof: See Appendix B. ■

Note that whenever ν_k increases, the solutions is more different than the original solution. Again, the computational complexity remains the same as the non-robust case.

C. Outdated CSI Considerations

The aforementioned robust design is able to support any kind of perturbation as long as it can be modelled by (1). Indeed, the more accurate the perturbation matrix $\Delta \mathbf{H}$ is modelled, the better performance will be obtained. Whenever the perturbations are created due to the mobility of the user terminals, there are several channel models available [30], [31] for determining a precise version of $\Delta \mathbf{H}$ can be obtained. Under this context, the channel modelling (2) can be reconsidered for mobile user terminals as

$$((\mathbf{A} + \Delta \mathbf{A})(\mathbf{G} + \Delta \mathbf{G})) \circ (\Phi + \Delta \Phi), \quad (55)$$

where $\Delta \mathbf{A}$, $\Delta \mathbf{G}$ and $\Delta \Phi$ models the fading, beam gain and path loss; and phase perturbation matrices. Although for $\Delta \mathbf{A}$ and $\Delta \mathbf{G}$ the system designer can consider certain mobility models and propose values depending on the user type (nomadic, maritime, etc), the mobility effect on the phase, $\Delta \Phi$ has not been studied yet.

Remarkably, the perturbation matrix due to the mobility effect strongly depends on the CSI feedback update rate. Precisely, $\Delta \mathbf{A}$, $\Delta \mathbf{G}$ and $\Delta \Phi$ are time-dependent so that the feedback rate and delay impacts the computation of the robust precoding design.

Operating (55) we can obtain

$$\Delta \mathbf{H} = \Delta (\mathbf{A}, \mathbf{G}) \circ \Phi + \mathbf{A} \mathbf{G} \circ \Delta \Phi + \Delta (\mathbf{A}, \mathbf{G}) \circ \Delta \Phi, \quad (56)$$

where

$$\Delta (\mathbf{A}, \mathbf{G}) = \mathbf{A} \Delta \mathbf{G} + \Delta \mathbf{A} \mathbf{G} + \Delta \mathbf{A} \Delta \mathbf{G}. \quad (57)$$

Consequently, in order to evaluate the performance of the robust scheme whenever mobile terminals are considered, exhaustive simulations shall be carried out in order to determine the maximum allowed mobility pattern and its corresponding feedback rate given a target average throughput per beam. These evaluations are out of the scope of this paper and they are left for further works.

V. USER GROUPING

One of the main limiting factors of multibeam multicast precoding is the spatial diversity of the users within each beam. Indeed, whenever the targeted users in each beam have orthogonal channel vectors, this is,

$$\mathbf{h}_{k,m}^H \mathbf{h}_{k,n} = 0, \quad (58)$$

for the k -th beam for $m, n = 1 \dots, Q$ and $m \neq n$; the intra-beam precoding is not able to deliver the intended symbols. Under this context it is beneficial that the system designer performs a user grouping before the precoding matrix is computed so that users with collinear channel vectors are simultaneously served. Note that collinear channel vectors generally correspond to geographically close user (i.e. similar beam gains) whenever the relative phase between them is low (i.e. $\theta_{q,n}^{ultra}$ is approximately equal for all n and for the two users).

A. k -User Grouping

In a given time instant, the scheduler determines a set of tentative users to be served. The number of these scheduled users is considered the same for each beam, fixed and equal to Q . For each beam, obtaining the most adequate groups of users is a cumbersome problem. Note that first, the system designer shall determine the adequate number of groups G_k per beam and, posteriorly, group them into those G_k groups. Clearly, the overall system throughput will depend on the user density over the coverage area: the larger number of users over the coverage, the larger throughputs can be obtained.

In order to solve this problem, we will consider a random pre-processing. This pre-processing consists of randomly choose a user from the beam and, posteriorly, obtain the group of users. Note that with this first processing, we are severely leveraging the computational complexity of the technique.

Under this context, let us consider that we have elected an arbitrary user m within the k -th beam. The user grouping

scheme shall obtain the closest $Q - 1$ users in terms of Euclidean norm. Mathematically,

$$\begin{aligned} & \underset{n \in 1, \dots, Q}{\text{minimize}} \quad \|\mathbf{h}_{k,m} - \mathbf{h}_{k,n}\|^2 \\ & \text{subject to} \\ & n \neq m. \end{aligned} \quad (59)$$

Since the considered Q in (59) is not expected to be large, this optimization only requires a set of Euclidean norm comparisons between the scheduled users. As it happens with the precoding design, the user grouping scheme suffers from degradation whenever the user channel vectors are corrupted. A method for robustly grouping them is presented in the next subsection.

B. Robust k -User Grouping

Whenever the channel vectors are corrupted by a certain perturbation, a worst-case optimization shall be performed

$$\begin{aligned} & \underset{n \in 1, \dots, Q}{\text{minimize}} \quad \underset{\{\delta_{k,q}\}_{q=1}^Q}{\text{maximize}} \quad \|\mathbf{h}_{k,m} + \delta_{k,m} - \mathbf{h}_{k,n} - \delta_{k,n}\|^2 \\ & \text{subject to} \\ & n \neq m, \\ & \|\delta_{k,q}\|^2 \leq \gamma_{k,q}. \end{aligned} \quad (60)$$

Next theorem provides an approximate version of the aforementioned problem.

Theorem 3 *An optimization problem whose solutions upper bound the original worst-case robust grouping problem (60) is*

$$\begin{aligned} & \underset{n \in 1, \dots, Q}{\text{minimize}} \quad \|\mathbf{h}_{k,m} - \mathbf{h}_{k,n}\|^2 + \gamma_{n,q} \\ & \text{subject to} \\ & n \neq m. \end{aligned} \quad (61)$$

Proof: It is a simple derivation considering the Cauchy-Schwarz inequality and the fact that given a randomly chosen user m its perturbation does not influence the grouping optimization. ■

With this optimization it is evident that whenever uncertainty is assumed in the channel vectors, this shall be considered in the user grouping design by means of an additional scalar penalty. Remarkably, in case we consider the same uncertainty to all users, the proposed approximate solution remains the same.

VI. MULTIPLE GATEWAY ARCHITECTURE

As a matter of fact, there might be the case where the feeder link cannot support the overall satellite data traffic. For instance, a payload equipped with $N = 155$ feeds with a user channel bandwidth of 500 MHz requires a feeder link bandwidth of 77.5 GHz which is an unaffordable requirement even if the feeder link carrier is located at the Q/V band.

In order to solve this problem, the feeder link might benefit from certain spatial reuse so that several gateways can simultaneously send the data to be transmitted over the satellite

coverage area. Under this context, G gateways can reuse the available bandwidth for the feeder link leading to large increase of the user bandwidth (see Figure 2). However, in a multiple gateway scenario, the precoding scheme shall be reconsidered.

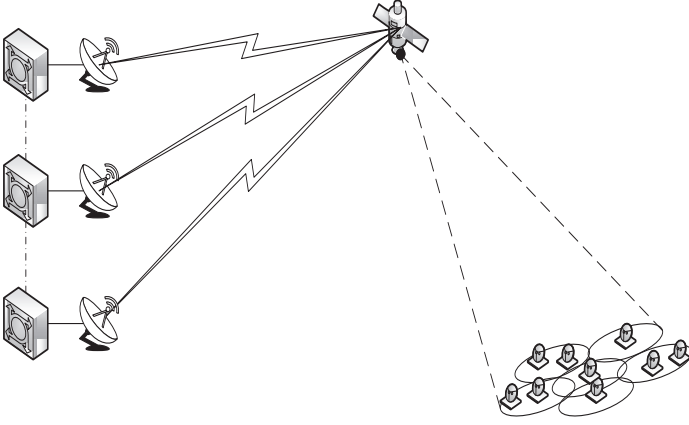


Fig. 2. The picture depicts the multiple gateway multicast multibeam satellite structure. In contrast to the single gateway architecture, several gateways transmit the data to be delivered to the coverage area. This entails two main drawbacks. First, certain inter-gateway link (dotted lines) shall exist. Second, each ground unit must compute an independent submatrix of the overall precoding matrix.

In order to keep the payload complexity low, each feeder link receiver at the payload will only route signals a set of feeds N_g for $g = 1, \dots, G$. Otherwise, a very complex analog scheme shall be implemented. In addition, it is important to remark that the feeder link bandwidth resources can only support a small number of N_g feed signals. Considering this approach, the precoding matrix \mathbf{W} must be partitioned into G sub-matrices leading to a large decrease of the achievable throughput. In the following subsections we propose some techniques in order to overcome this limitation.

In addition, considering that in order to reduce the inter-gateway communication, each gateway individually computes its precoding sub-matrix, certain cooperative scheme shall be conceived. Indeed, each gateway only have access to the feedback from its corresponding set of feeds N_g . With this, certain CSI cooperation among gateways shall be established so that inter-beam interference is mitigated.

A. Precoding Scheme

As discussed in the previous section, the g -th gateway only has access to a set of N_g of the overall feed elements located at the payload. Additionally, the gateway serves a set of K_g beams out of the K , leading to a total amount of served users equal to $K_g Q$. We will assume a known feed allocation per gateway and fixed N_g and K_g . Precisely, we will consider that the feeds are assigned in a consecutive fashion over the channel matrix as it is defined in the following.

Let us assume that each gateway has access to the overall CSI. With this, the matrix to be transmitted through the feeder

link of the g -th gateway jointly with the user symbols is

$$\mathbf{W}^g \in \mathbb{C}^{N_g \times K_g}. \quad (62)$$

In other words, as each gateway only have access to a certain set of feed elements the symbols to be transmitted to the K_g beams shall be linearly transformed with \mathbf{W}^g in order to increase the overall throughput. Whenever each gateway has access to the overall channel matrix \mathbf{H} , the precoding scheme can be computed as described in Section III and adapted to the multiple gateway scenario. This can be done by beams of setting zero entries in the precoding matrix whenever the gateway does not have access to a certain feed. This transformation leads to a block diagonal precoding matrix as follows

$$\mathbf{W}_{\text{M-GW}} = \begin{bmatrix} \mathbf{W}^1 & \mathbf{0} & \dots & \mathbf{0} \\ \mathbf{0} & \mathbf{W}^2 & \dots & \mathbf{0} \\ \vdots & \vdots & \ddots & \vdots \\ \mathbf{0} & \mathbf{0} & \dots & \mathbf{W}^G \end{bmatrix} \in \mathbb{C}^{N \times K}. \quad (63)$$

Evidently, robust designs can be applied without any additional penalty.

B. CSIT Sharing

Since the gateway only has access to certain beams, its available CSI is reduced. Precisely, the g -th receives from its feedback link the following matrix

$$\mathbf{H}^g = \mathbf{H}(((g-1)QK_g + 1) : gQK_g, 1 : N) \in \mathbb{C}^{QK_g \times N_g}, \quad (64)$$

where the Matlab notation has been used for the sake of clarity. However, in order to compute the precoding matrix, the gateways need the channel effect between their assigned feeds to the non-intended users. With this, every gateway must transmit over the inter-gateway link (e.g. a fiber optic) the information fed back from its users corresponding the effect of the non-assigned feeds. Mathematically, the g -th gateway must share

$$(\mathbf{H}^{g_l})_{l \neq g}^G, \quad (65)$$

where

$$\mathbf{H}^{g_l} = \mathbf{H}(((g-1)QK_g + 1) : gQK_g, ((l-1)N_g + 1) : gN_g). \quad (66)$$

This cooperation among gateways require a total amount of

$$(G-1)QK_gN_g \quad (67)$$

complex numbers to be shared by each gateway. As a consequence, it is essential to reduce this communication overhead in order to reduce the overall system cost.

One approach is to limit the sharing between the different gateways and only consider the C closer gateways. Note that we understand by 'close' gateways the ones which serve consecutive clusters in the channel matrix. Clearly, this might not correspond to geographically close gateways. With this, the overall data overhead reduces to

$$CQK_gN_g. \quad (68)$$

Another alternative is to apply certain compression to the transmit channel submatrices. For instance, we could use the eigenvector associated to the largest eigenvalue of each matrix \mathbf{H}^{g_i} . This will lead to a total communication overhead of

$$(G - 1)N_g. \quad (69)$$

Evidently, whenever each gateway has a more precise version of the channel matrix, the larger throughput can be obtained. In the simulation section this is evaluated and different cooperation schemes are evaluated.

VII. SIMULATIONS

Disclaimer: The produced results are indicative and might not hold for other channel types and algorithm configurations. A more accurate evaluation of the performance of the methods proposed herein is out of the scope of this work.

TABLE I. USER LINK SIMULATION PARAMETERS

Parameter	Value
Satellite height	35786 km (geostationary)
Satellite longitude, latitude	$10^\circ \text{ East}, 0^\circ$
Earth radius	6378.137 Km
Feed radiation pattern	Provided by ESA [22]
Number of feeds N	245
Beamforming matrix \mathbf{B}	Provided by ESA [22]
Number of beams	245
User location distribution	Uniformly distributed
Carrier frequency	20 GHz (Ka band)
Total bandwidth (B)	500 MHz
Roll-off factor (α)	0.25
User antenna gain	41.7 dBi
G/T	17.68 dB/K

Considering a reference scenario of a geostationary satellite with $N = K = 245$, we evaluate the proposed precoding designs considering a full frequency reuse scenario. Array fed radiation pattern has been provided by the European Space Agency and it takes into account the different user locations over the European continent. The link budget parameters are described in Table 1.

All results have been obtained considering 500 channel realizations and a phase effect between feeds $\chi^2 = 10$ degrees. Remarkably, it has been observed that the channel realizations is sufficiently large for providing converged results. Moreover, throughput values are obtained by means of the user SINR and the efficiency (bit/symbol) given a minimum Packet Error Rate (PER) of 10^{-6} considering DVB-S2X. It is important to remark that this relationship has been obtained from [32] considering the PER curves. With this, the DVB-S2X throughput for the k -th beam becomes

$$R_{\text{DVB-S2X},k} = \min_{q=1,\dots,Q} \frac{2B}{1+\alpha} f_{\text{DVB-S2X}}(\text{SINR}_{k,q}), \quad (70)$$

where $f_{\text{DVB-S2X}}(\cdot)$ is function that provides the DVB-S2X spectral efficiency for a given SINR.

The outline of the subsequent subsections is as follows. First, we show the performance gain of the proposed precoding schemes considering perfect CSI and single gateway architecture. Second, it is shown that larger throughputs can be obtained if user grouping techniques are applied. Third,

the impact of imperfect CSI is shown and the convenience of robust designs is presented. Finally, the multiple gateway architecture is evaluated so as the proposed inter-gateway cooperation techniques. Remarkably, for a best practice we also consider a reference scenario that consists in 4-colouring scheme where the interference is reduced so as the available bandwidth.

Figure 3 presents the system throughput considering the proposed precoding schemes in section III. Both of them, R-ZF and MBIM are compared to the average MMSE design presented in [16], [33] and the frame-based precoding approach presented in [18]. It can be observed that both proposals behave better than average MMSE scheme. Specially, MBIM offers larger throughputs than R-ZF over the different transmit power values. Remarkably, MBIM scheme offers slightly higher average throughput performance per beam than the frame-based design [18] denoted as SRM. Moreover, the conventional 4-coloring scheme has the lowest achievable rate due to the bandwidth limitations. For this concrete scenario, MBIM can offer a throughput increase of at least 1.5% with respect to the SRM scheme while offering a substantial computational complexity reduction. Considering that the authors implementation of SRM has not been cross-validated with the authors of [18] and the fact that the throughput techniques depend on the multibeam coverage area, we cannot infer that in general MBIM offers higher achievable rates than SRM. The shown comparative results just aim at illustrating the potential competitive performance of the proposed technique. It is not the goal to conclude that it is a better or worst technique in terms of rate. A complete comparison would require the evaluation of both algorithms over a myriad of scenarios. This comparison is out of the scope of this paper. In any case, as it is presented in the previous sections, MBIM presents a reduced computational complexity, it is able to deal with a multigateway architecture and a robust version of the scheme can be applied without increasing the computational complexity.

It is important to state that the average throughput per beam is reduced as the number of users per beam, Q , increases. This effect can be further observed in figure 4. It can be observed that for the R-ZF and the MBIM precoding techniques offer higher spectral efficiencies than the 4-colour case for even 5 users per frame. On the contrary, the average MMSE technique shows a poor performance for $Q \geq 4$.

As an additional comparison metric, we evaluate the average computational time. Table II depicts the obtained results by averaging over 10 realizations with a Windows desktop with 12 Intel i5 cores and 16GB of RAM. It can be observed that MBIM shows a 3-fold performance gain in terms of computational time. To implement SRM, we used CVX 2.0 64 bit a package for specifying and solving convex programs [34], [35]

A. User Grouping

As discussed before, whenever the users within the same beam have collinear channel vectors, large rates can be obtained. This is shown in Figure 5. Similar to the study in [4], in each beam $Q = 200$ users are uniformly distributed, resulting

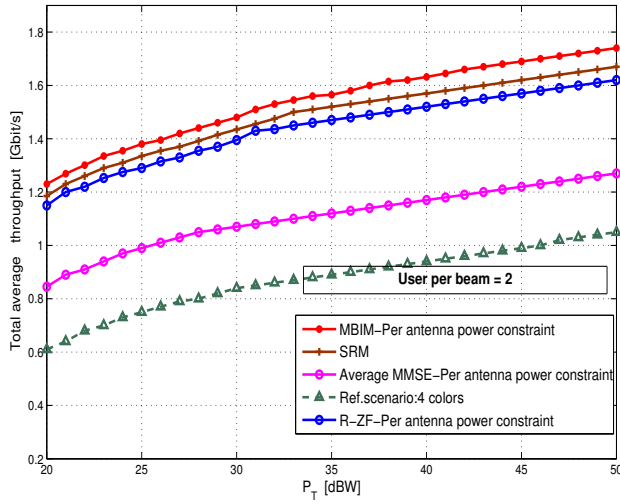
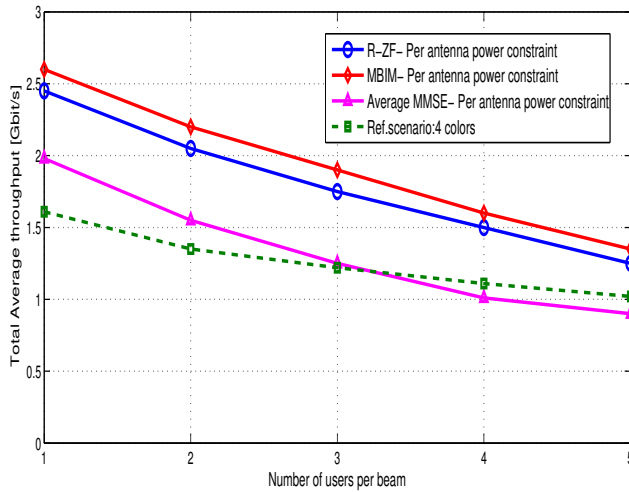
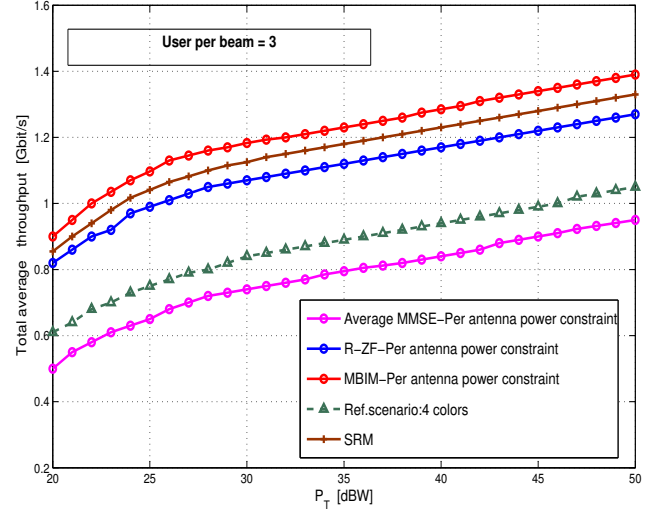

 Fig. 3. Per beam average throughput with $Q = 2, 3$ users per beam.


Fig. 4. Per beam average throughput when the number of users per beam varies.

TABLE II. SIMULATION TIME TABLE FOR A SET OF 10 REALIZATIONS

User per beam	Average Time/sec MBIM—SRM	Normalized time
Q=1	12.972—65.354	5.06
Q=2	29.346—94.866	3.2
Q=3	32.685—125.013	3.8
Q=4	38.635—143.269	3.7

in an average user density of 0.023 users/km^2 inside the 3 dB coverage edge of every beam.

It results that in all cases, user grouping increases the throughput. Specifically, for $Q = 3$, the user grouping gain becomes larger than in the $Q = 2$ case. Considering that for the MBIM the user grouping can increase the average throughput per beam at least 12%, it results convenient to implement this

technique in satellite systems. It is important to remark that whenever scheduling algorithms are employed jointly with the precoding design as in [18], very high gains can be achieved compared to the presented in this section.

B. Robust Design

This subsection considers the effect of imperfect CSI at the transmitter. This is modelled with a additive perturbation matrix whose entries are Gaussian distributed with zero mean and variance equal to 1. The perturbation values γ_k are considered the same for all submatrices ($K = 1, \dots, K$) and in the simulations are obtained considering that each submatrix does no exceed the assumed bound. Additionally, γ_k is set to 1 and no sensitivity analysis is performed due to space limitations.

Figure 6 shows the performance of our proposal for different γ values represented in a ratio basis with respect to the channel matrix Frobenious norm. For both cases $Q = 2, 3$, the proposed technique is able to overcome the imperfect CSI values at the transmitter leading to an increase of the throughput from 0.5% to the 3% while keeping the precoding complexity low.

C. Multiple Gateway Transmission

In order to evaluate the performance of the proposed multiple gateway schemes, we consider the following methods and inter-gateway architectures. We will consider a total number of $G = 14$ gateways each of them serving either 17 or 18 beams.

- **Scenario 1 :** Individual cluster processing. Each gateway processes its set of beams independently and only receives the CSI from its corresponding beams. With this, it is not possible to mitigate the interference of adjacent beams. This is referred to Individual Cluster Processing (ICP).

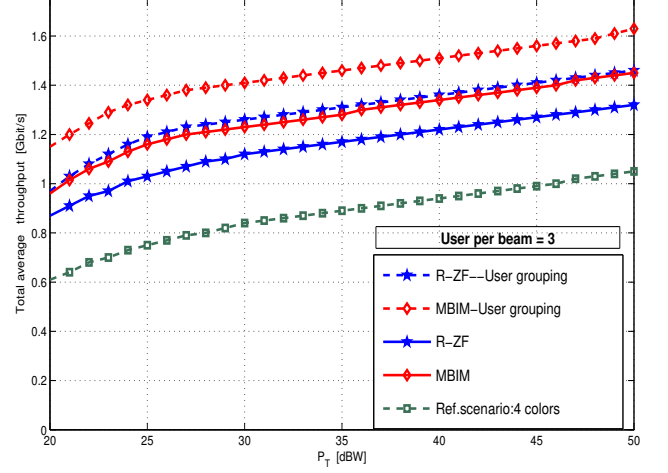
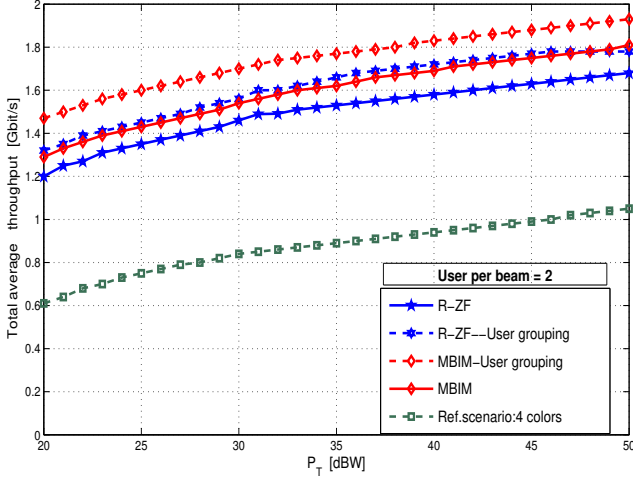


Fig. 5. Per beam average throughput with $Q = 2, 3$ users, perfect CSI, user grouping.

- **Scenario 2 :** Gateway g (respectively for all the gateways) collaborates with 4 gateways that serve beams directly adjacent to their beams so that g -th gateway receives perfect CSI of adjacent beams. This is referred to 4 Gateway Collaboration Processing (4GCP).
- **Senario 3 :** Gateway g (respectively for all the gateways) collaborates with 7 gateways that serve beams directly adjacent to their beams so that g -th gateway receives perfect CSI of adjacent beams. This is referred to 7 Gateway Collaboration Processing (7GCP).
- **Senario 4 :** Gateway g (respectively for all the gateways) collaborates with all gateways by means of sharing the singular left vector associated with the largest singular value of the gateway channel matrix. This is referred to Maximum SVD of Gateway Collaboration (MSVDGC).
- **Senario 5 :** Single gateway scenario so that a unique on ground processing unit is able to use all available feeds with the overall channel matrix. This scenario refers to Reference scenario (Ref).

Figure 7 shows the proposed multiple gateway architectures for both the R-ZF and MBIM precoding designs. Evidently, as it happened in the single gateway scenario, MBIM provides larger overall throughputs than the R-ZF in all cases. In addition, it is observed that the larger cooperation is considered, the larger throughputs are obtained. Precisely, the MSVDGC method only shows a throughput loss of a 1.5 % over all transmit powers with respect to the ideal full cooperative case.

Remarkably, MSVDGC method offers a good trade-off between overall throughput and inter-gateway communication overhead. For the sake of completeness, Figure 8 depicts the average throughput per beam the of proposed precoding techniques when the number of users per beam, Q , increases.

VIII. CONCLUSIONS

This paper proposed a two-stage low complex precoding design for multibeam multicast satellite systems. While the

first stage minimizes the inter-beam interference, the second stage enhances the intra-beam SINR. A robust version of the proposed scheme is provided based on the novel approach of the first perturbation theory. Additionally, user grouping and multiple gateway schemes are presented as essential tools for increasing the throughput in multibeam satellite systems. The conceived methods are evaluated in a continental coverage area and they result to perform better than the current approaches yet offering a low computational complexity.

APPENDIX A PROOF OF THEOREM 1

After some manipulations, the objective function can be written

$$\sum_{k=1}^K \text{trace} \left(\mathbf{W}_{a_k}^H \left(\hat{\mathbf{H}}_k^H \hat{\mathbf{H}}_k + \frac{KQ}{P_T} \mathbf{I} \right) \mathbf{W}_{a_k} \right). \quad (71)$$

This objective function can be re-written considering the eigendecomposition of $\hat{\mathbf{H}}_k^H \hat{\mathbf{H}}_k = \hat{\mathbf{V}}_k \hat{\Sigma}_k \hat{\mathbf{V}}_k^H$, so that

$$\sum_{k=1}^K \text{trace} \left(\mathbf{W}_{a_k}^H \hat{\mathbf{V}}_k \left(\hat{\Sigma}_k + \frac{KQ}{P_T} \mathbf{I} \right) \hat{\mathbf{V}}_k^H \mathbf{W}_{a_k} \right). \quad (72)$$

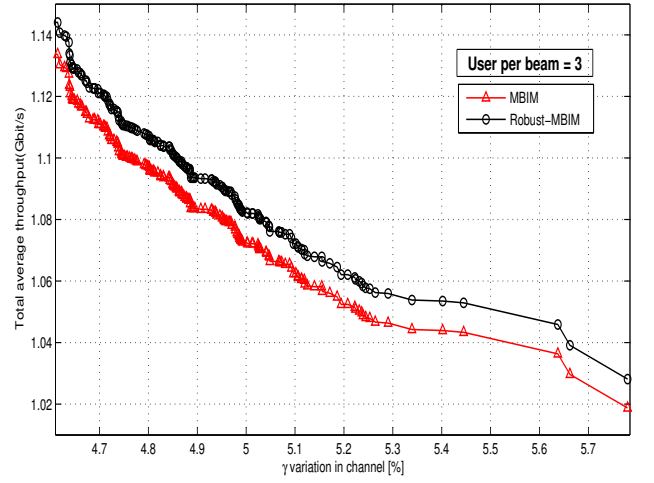
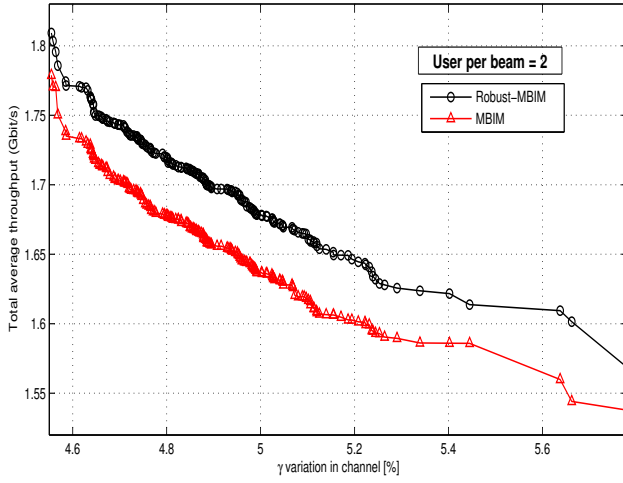
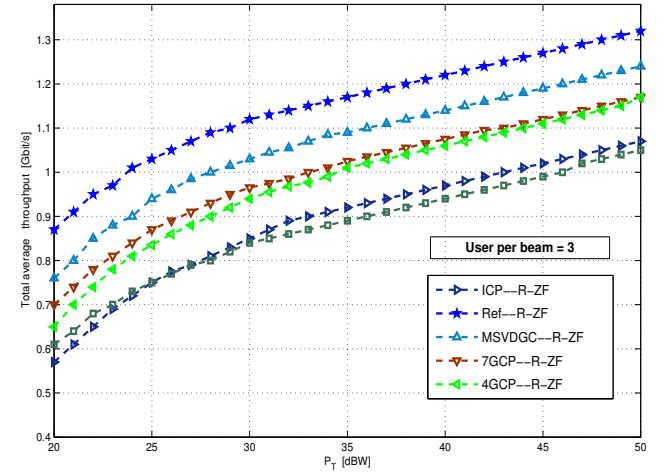
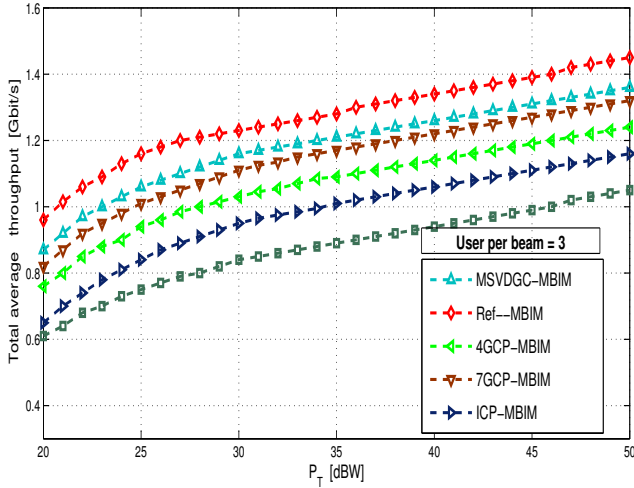
Since the objective function depends on the perturbation matrices and they are unknown by the transmitter, the following derivations aim at obtaining an upper-bound of (72). Concretely, an upper-bound of both $\hat{\mathbf{V}}_k$ and $\hat{\Sigma}_k$ will be presented. The optimization problem (19) can yield to a tractable solution.

Proceeding with the derivation, the following equality holds

$$\hat{\mathbf{H}}_k^H \hat{\mathbf{H}}_k = \tilde{\mathbf{H}}_k^H \tilde{\mathbf{H}}_k + \tilde{\Delta}_k^H \tilde{\mathbf{H}}_k + \tilde{\mathbf{H}}_k^H \tilde{\Delta}_k + \tilde{\Delta}_k^H \tilde{\Delta}_k, \quad (73)$$

where it can be observed that the first term is the exact term whereas the rest are perturbation terms. In the following, we will consider the perturbation effect of

$$\Delta \mathbf{K}_k = \tilde{\Delta}_k^H \tilde{\mathbf{H}}_k + \tilde{\mathbf{H}}_k^H \tilde{\Delta}_k + \tilde{\Delta}_k^H \tilde{\Delta}_k, \quad (74)$$


 Fig. 6. Per beam average throughput with $Q = 2, 3$ users, imperfect CSI, no user grouping.

 Fig. 7. Per beam average throughput with $Q = 3$ users, perfect CSI, no user grouping and different multiple gateway architectures with MBIM precoding (Left), R-ZF precoding(Right).

in the precoding design.

Considering the first order perturbation analysis presented in [20], the eigenvectors of $\hat{\mathbf{H}}_k^H \hat{\mathbf{H}}_k$ can be written as

$$\hat{\mathbf{V}}_k = \tilde{\mathbf{V}}_k (\mathbf{R}_k + \mathbf{I}), \quad (75)$$

where

$$\mathbf{R}_k = \mathbf{D} \circ \left(\tilde{\mathbf{V}}_k^H \Delta \mathbf{K} \tilde{\mathbf{V}}_k \tilde{\Sigma}_k + \tilde{\Sigma}_k \tilde{\mathbf{V}}_k^H \Delta \mathbf{K}^H \tilde{\mathbf{V}}_k \right). \quad (76)$$

where the g, f -entry of \mathbf{D} is

$$\frac{1}{\lambda_f - \lambda_g}, \quad (77)$$

for $f \neq g$ and 0 whenever $f = g$. λ_f denotes the f -th eigenvalue of $\hat{\mathbf{H}}_k^H \hat{\mathbf{H}}_k$. It is important to remark that it has been considered that $\hat{\mathbf{H}}_k^H \hat{\mathbf{H}}_k$ is full rank and, therefore, its null space has 0 dimension.

From the problem definition (19) it is possible to bound $\Delta \mathbf{K}$ such that

$$\Delta \mathbf{K}_k \preceq \left(\hat{\gamma}_k^2 + 2\hat{\gamma}_k \sigma_{\max} \left(\tilde{\mathbf{H}}_k^H \tilde{\mathbf{H}}_k \right) \right) \mathbf{I}. \quad (78)$$

With this and considering the following lemma:

Lemma 1. For any semidefinite positive square matrices $\mathbf{A}, \mathbf{B}, \mathbf{C}$ and $\mathbf{B} \preceq \mathbf{C}$ it holds that

$$\mathbf{A} \circ \mathbf{B} \preceq \mathbf{A} \circ \mathbf{C} \quad (79)$$

Proof: See Theorem 17 of [36]. ■

It is possible to write the following inequality

$$\hat{\mathbf{V}}_k \preceq \tilde{\mathbf{V}}_k \left(\hat{\mathbf{R}}_k + \mathbf{I} \right), \quad (80)$$

where

$$\hat{\mathbf{R}}_k = \epsilon_k \mathbf{D} \circ \left(\tilde{\mathbf{V}}_k^H \tilde{\mathbf{V}}_k \tilde{\Sigma}_k + \tilde{\Sigma}_k \tilde{\mathbf{V}}_k^H \tilde{\mathbf{V}}_k \right), \quad (81)$$

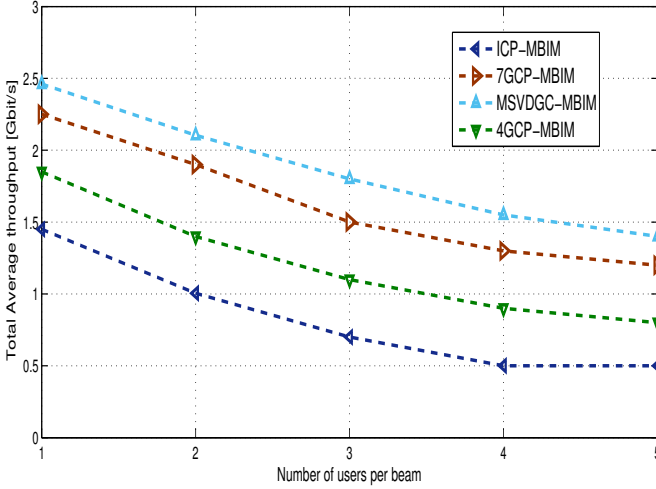


Fig. 8. Per beam average throughput in multiple gateway-multicast scenario when the number of users per beam varies.

where

$$\epsilon = \hat{\gamma}_k^2 + 2\hat{\gamma}_k\sigma_{\max} \left(\tilde{\mathbf{H}}_k^H \tilde{\mathbf{H}}_k \right) \quad (82)$$

In case the perturbations of the eigenvectors are consider, the Weyl's inequality can support the approximation

Lemma 2 (Weyl's inequality) Given two Hermitian semidefinite positive matrices \mathbf{A}_1 and \mathbf{A}_2 with their corresponding eigenvalues collapsed in the diagonal matrices Σ_1 , Σ_2 , the following inequality holds

$$\Sigma_{\text{sum}} \preceq \Sigma_1 + \Sigma_2, \quad (83)$$

where Σ_{sum} is a diagonal matrix whose diagonal entries are the eigenvalues of $\mathbf{A}_1 + \mathbf{A}_2$.

Proof: See [37]. ■

With this, the eigenvalues of $\tilde{\mathbf{H}}_k^H \tilde{\mathbf{H}}_k$ can be upper-bounded so that

$$\hat{\Sigma}_k \preceq \tilde{\Sigma}_k + \epsilon_k \mathbf{I}. \quad (84)$$

With both (80) and (84), it is possible to relax the worst-case maximization in (46). In other words, it is possible to use (80) and (84) as eigendecomposition of matrix $\hat{\mathbf{H}}_k$.

APPENDIX B PROOF OF THEOREM 2

As for the previous theorem, the main objective is to find a bound of the objective function so that the dependence with respect to Δ_k variable disappears.

Considering the first order perturbation model presented in [20], the required eigendecomposition of $\mathbf{H}_k \mathbf{W}_{a_k}$ is perturbed by the following matrix

$$\Delta \mathbf{Q}_k = \Delta_k \mathbf{W}_{a_k}. \quad (85)$$

This leads to the following approximation of the eigenvectors of \mathbf{Z}_k

$$\hat{\mathbf{Z}}_k = \mathbf{L}_k (\mathbf{M}_k + \mathbf{I}), \quad (86)$$

where \mathbf{L}_k are the eigenvectors of \mathbf{Z}_k and

$$\mathbf{M}_k = \mathbf{N} \circ (\mathbf{L}_k^H \Delta \mathbf{Q}_k \mathbf{L}_k^H \mathbf{T}_k + \mathbf{T}_k \mathbf{L}_k^H \Delta \mathbf{Q}_k \mathbf{L}_k) \quad (87)$$

where \mathbf{T}_k is a diagonal matrix containing the eigenvalues of \mathbf{Z}_k and the g, f -th entry of \mathbf{N} is

$$\frac{1}{z_{k_f} - z_{k_g}}, \quad (88)$$

for $f \neq g$ and 0 whenever $f = g$. z_{k_f} denotes the f -th eigenvalue of \mathbf{Z}_k .

After some manipulations, we can lower-bound $\Delta \mathbf{Q}_k$ so that

$$\Delta \mathbf{Q}_k \succeq \underline{\gamma}_k \mathbf{1}^T \left(\tilde{\Sigma}_k + \epsilon_k \mathbf{I} \right)^{-1/2} \mathbf{1} \mathbf{I}. \quad (89)$$

By means of employing this last inequality and the derivation of the previous appendix, a lower bound of the eigenvalues of $\hat{\mathbf{Z}}_k$ can be established.

ACKNOWLEDGMENT

The authors would like to thank Pantelis-Daniel M. Arapoglou and the anonymous reviewers for their fruitful comments and discussions.

REFERENCES

- [1] A. Osseiran, F. Boccardi, V. Braun, K. Kusume, P. Marsch, M. Maternia, O. Queseth, M. Schellmann, H. Schotten, H. Taoka, H. Tullberg, M. Uusitalo, B. Timus, and M. Fallgren, "Scenarios for 5G mobile and wireless communications: the vision of the METIS project," *Communications Magazine, IEEE*, vol. 52, no. 5, pp. 26–35, May 2014.
- [2] B. Evans, "The role of satellites in 5G," in *Advanced Satellite Multimedia Systems Conference and the 13th Signal Processing for Space Communications Workshop (ASMS/SPSC)*, 2014 7th, Sept 2014, pp. 197–202.
- [3] J. Tronc, P. Angeletti, N. Song, M. Haardt, J. Arendt, and G. Gallinaro, "Overview and comparison of on-ground and on-board beamforming techniques in mobile satellite service applications," *International Journal of Satellite Communications and Networking*, vol. 32, no. 4, pp. 291–308, 2014. [Online]. Available: <http://dx.doi.org/10.1002/sat.1049>
- [4] P. M. Arapoglou, A. Ginesi, S. Cioni, S. Erl, F. Clazzer, S. Andrenacci, and A. Vanelli-Coralli, "DVB-S2x Enabled Precoding for High Throughput Satellite Systems," *CoRR*, vol. abs/1504.03109, 2015. [Online]. Available: <http://arxiv.org/abs/1504.03109>
- [5] L. Cottatellucci, M. Debbah, E. Casini, R. Rinaldo, R. Mueller, M. Neri, and G. Gallinaro, "Interference mitigation techniques for broadband satellite system," in *ICSSC 2006, 24th AIAA International Communications Satellite Systems Conference, 11-15 June 2006, San Diego, USA, San Diego, UNITED STATES, 06 2006*. [Online]. Available: <http://www.eurecom.fr/publication/1886>
- [6] J. Arnau, B. Devillers, C. Mosquera, and A. Perez-Neira, "Performance study of multiuser interference mitigation schemes for hybrid broadband multibeam satellite architectures," *EURASIP Journal on Wireless Communications and Networking*, vol. 2012, no. 1, p. 132, 2012. [Online]. Available: <http://jwcn.eurasipjournals.com/content/2012/1/132>
- [7] B. Devillers, A. Perez-Neira, and C. Mosquera, "Joint Linear Precoding and Beamforming for the Forward Link of Multi-Beam Broadband Satellite Systems," in *Global Telecommunications Conference (GLOBECOM 2011)*, 2011 IEEE, Dec 2011, pp. 1–6.
- [8] G. Zheng, S. Chatzinotas, and B. Ottersten, "Generic Optimization of Linear Precoding in Multibeam Satellite Systems," *Wireless Communications, IEEE Transactions on*, vol. 11, no. 6, pp. 2308–2320, June 2012.

- [9] D. Christopoulos, S. Chatzinotas, G. Zheng, J. Grotz, and B. Ottersten, "Linear and nonlinear techniques for multibeam joint processing in satellite communications," *EURASIP Journal on Wireless Communications and Networking*, vol. 2012, no. 1, p. 162, 2012. [Online]. Available: <http://jwcn.eurasipjournals.com/content/2012/1/162>
- [10] V. Joroughi, B. Devillers, M. Á. Vázquez, and A. I. Pérez-Neira, "Design of an on-board beam generation process for the forward link of a multi-beam broadband satellite system," in *2013 IEEE Global Communications Conference, GLOBECOM 2013, Atlanta, GA, USA, December 9-13, 2013*, 2013, pp. 2921–2926. [Online]. Available: <http://ieeexplore.ieee.org/xpl/articleDetails.jsp?arnumber=6831518>
- [11] A. Gharanjik, B. Shankar, P.-D. Arapoglou, and B. Ottersten, "Multiple Gateway Transmit Diversity in Q/V Band Feeder Links," *Communications, IEEE Transactions on*, vol. 63, no. 3, pp. 916–926, March 2015.
- [12] B. Devillers and A. Perez-Neira, "Advanced interference mitigation techniques for the forward link of multi-beam broadband satellite systems," in *Signals, Systems and Computers (ASIOMAR), 2011 Conference Record of the Forty Fifth Asilomar Conference on*, Nov 2011, pp. 1810–1814.
- [13] V. Joroughi, M. A. Vazquez, A. Perez-Neira, and A. Perez-Neira, "Multiple Gateway Precoding with Per Feed Power Constraints for Multibeam Satellite Systems," in *European Wireless 2014; 20th European Wireless Conference; Proceedings of*, May 2014, pp. 1–7.
- [14] G. Zheng, S. Chatzinotas, and B. Ottersten, "Multi-gateway cooperation in multibeam satellite systems," in *Personal Indoor and Mobile Radio Communications (PIMRC), 2012 IEEE 23rd International Symposium on*, Sept 2012, pp. 1360–1364.
- [15] N. Zorba, M. Realp, and A. I. Perez-Neira, "An improved partial CSIT random beamforming for multibeam satellite systems," in *Signal Processing for Space Communications, 2008. SPSC 2008. 10th International Workshop on*, Oct 2008, pp. 1–8.
- [16] G. Taricco, "Linear Precoding Methods for Multi-Beam Broadband Satellite Systems," in *European Wireless 2014; 20th European Wireless Conference; Proceedings of*, May 2014, pp. 1–6.
- [17] Y. Silva and A. Klein, "Linear Transmit Beamforming Techniques for the Multigroup Multicast Scenario," *Vehicular Technology, IEEE Transactions on*, vol. 58, no. 8, pp. 4353–4367, Oct 2009.
- [18] D. Christopoulos, S. Chatzinotas, and B. Ottersten, "Multicast Multi-group Precoding and User Scheduling for Frame-Based Satellite Communications," *Wireless Communications, IEEE Transactions on*, vol. PP, no. 99, pp. 1–1, 2015.
- [19] V. Stankovic and M. Haardt, "Generalized Design of Multi-User MIMO Precoding Matrices," *Wireless Communications, IEEE Transactions on*, vol. 7, no. 3, pp. 953–961, March 2008.
- [20] J. Liu, X. Liu, and X. Ma, "First-Order Perturbation Analysis of Singular Vectors in Singular Value Decomposition," *Signal Processing, IEEE Transactions on*, vol. 56, no. 7, pp. 3044–3049, July 2008.
- [21] M. Schneider, C. Hartwanger, and H. Wolf, "Antennas for multiple spot beam satellites," *CEAS Space Journal*, vol. 2, no. 1-4, pp. 59–66, 2011. [Online]. Available: <http://dx.doi.org/10.1007/s12567-011-0012-z>
- [22] ESA, "Next Generation Waveforms for Improved Spectral Efficiency: Candidate Techniques for FWD Link Air Interface Enhancements. European Space Agency Contract: 4000106528/12/NL/NR," 2013.
- [23] M. Aloisio and P. Angeletti, "Multi-Amplifiers Architectures for Power Reconfigurability," in *Vacuum Electronics Conference, 2007. IVEC '07. IEEE International*, May 2007, pp. 1–2.
- [24] J. Lizarraga, P. Angeletti, N. Alagha, and M. Aloisio, "Flexibility performance in advanced Ka-band multibeam satellites," in *Vacuum Electronics Conference, IEEE International*, April 2014, pp. 45–46.
- [25] E. Karipidis, N. Sidiropoulos, and Z.-Q. Luo, "Transmit beamforming to multiple co-channel multicast groups," in *Computational Advances in Multi-Sensor Adaptive Processing, 2005 1st IEEE International Workshop on*, Dec 2005, pp. 109–112.
- [26] G. H. Golub and C. F. Van Loan, *Matrix Computations (3rd Ed.)*. Baltimore, MD, USA: Johns Hopkins University Press, 1996.
- [27] T. H. Cormen, C. Stein, R. L. Rivest, and C. E. Leiserson, *Introduction to Algorithms*, 2nd ed. McGraw-Hill Higher Education, 2001.
- [28] A. Pascual-Iserte, D. Palomar, A. Perez-Neira, and M. Lagunas, "A robust maximin approach for MIMO communications with imperfect channel state information based on convex optimization," *Signal Processing, IEEE Transactions on*, vol. 54, no. 1, pp. 346–360, Jan 2006.
- [29] D. Palomar, *A Unified framework for communications through MIMO channels*, Phd Dissertation, 2003.
- [30] F. Fontan, M. Vazquez-Castro, C. Cabado, J. Garcia, and E. Kubista, "Statistical modeling of the LMS channel," *Vehicular Technology, IEEE Transactions on*, vol. 50, no. 6, pp. 1549–1567, Nov 2001.
- [31] K. Liolis, J. Gomez-Vilardebo, E. Casini, and A. Perez-Neira, "Statistical Modeling of Dual-Polarized MIMO Land Mobile Satellite Channels," *Communications, IEEE Transactions on*, vol. 58, no. 11, pp. 3077–3083, November 2010.
- [32] "Digital Video Broadcasting (DVB); Second generation framing structure, channel coding and modulation systems for Broadcasting, Interactive Services, News Gathering and other broadband satellite applications; Part 2: DVB-S2 Extensions (DVB-S2X)," *ETSI EN 302 307-2*, 2014.
- [33] D. Christopoulos, S. Chatzinotas, and B. Ottersten, "Frame based precoding in satellite communications: A multicast approach," in *Advanced Satellite Multimedia Systems Conference and the 13th Signal Processing for Space Communications Workshop (ASMS/SPSC), 2014 7th*, Sept 2014, pp. 293–299.
- [34] M. Grant and S. Boyd, "CVX: Matlab software for disciplined convex programming, version 2.1," <http://cvxr.com/cvx>, Mar. 2014.
- [35] —, "Graph implementations for nonsmooth convex programs," in *Recent Advances in Learning and Control*, ser. Lecture Notes in Control and Information Sciences, V. Blondel, S. Boyd, and H. Kimura, Eds. Springer-Verlag Limited, 2008, pp. 95–110, http://stanford.edu/~boyd/graph_dcp.html.
- [36] C. R. Johnson, "Partitioned and Hadamard Product Matrix Inequalities," *JOURNAL OF RESEARCH of the National Bureau of Standards*, vol. 83, no. 6, pp. 3044–3049, November 1978.
- [37] H. Weyl, "Das asymptotische Verteilungsgesetz der Eigenwerte linearer partieller Differentialgleichungen (mit einer Anwendung auf die Theorie der Hohlraumstrahlung)," *Mathematische Annalen*, vol. 71, no. 4, pp. 441–479, 1912. [Online]. Available: <http://dx.doi.org/10.1007/BF01456804>



Vahid Joroughi was born in 1980, Mianeh, Iran. He received his Bachelor and Master degrees in Electrical Engineering in his home country within 2003-2009. During the same time, he also joined Iran Telecommunication Company (ITC) as a switching manager in order to participate in "NEAX" project jointly supported by ITC and NEC Company. From January 2012 to December 2015, he was awarded with the FPU-UPC grant to conduct his PhD studies jointly at the Centre Tecnològic de Telecomunicacions de Catalunya (CTTC) and Universidad Politècnica de Catalunya (UPC), Barcelona. His PhD program has been done in the context of different projects provided by European Space Agency (ESA) on the topic of Multibeam Satellite Communication network. He is currently holds a postdoctoral position at Universidad de Vigo. His research interest includes Satellite Communications with special emphasis on MIMO satellite infrastructure, Statistical/array signal processing and cooperative communication.



Miguel Ángel Vázquez was born in Palma de Mallorca, Spain, in 1986. He received the Telecommunication Engineering degree from the TelecomBCN Technical University of Catalonia (UPC), his master degree on research on wireless communication (MERIT) in 2012. He has completed his Phd in telecommunications in 2014 from UPC, leading to a Phd thesis title Beamforming and Power Control in Spectrum Sharing Systems. He joined the CTTC in January 2010. He has been granted with a Marie Curie fellowship in the context of a FP7 european

project (SWAP). Moreover, he has participated in different EU-funded projects (FP7, ARTEMISA, CELTIC, H2020) on the topics of internet of things and smart grid; and, another industrial contracts with local companies and the European Space Agency. His research interests include statistical and array signal processing, spectrum sharing wireless communications, licensed shared access networks, satellite communications. He is co-organizing IEEE ASMS-SPSC 2016 Conference and IEEE S3P Summer School in Signal Processing for Satellite Communications.



Ana I. Pérez-Neira (IEEE Senior member: 03082260) is full professor at UPC (Technical University of Catalonia) in the Signal Theory and Communication department. Her research topic is signal processing for communications and currently she is working in multi-antenna and multicarrier signal processing, both, for satellite communications and wireless systems. She has been in the board of directors of ETSETB (Telecom Barcelona) from 2000-03 and Vicerector for Research at UPC (2010-13). She created UPC Doctoral School (2011). Currently, she

is Scientific Coordinator at CTTC (Centre Tecnològic de Telecomunicacions de Catalunya). Since 2008 she is member of EURASIP BoD (European Signal Processing Association) and since 2010 of IEEE SPTM (Signal Processing Theory and Methods). She is the coordinator of the European project SANSA and of the Network of Excellence on satellite communications, financed by the European Space Agency: SatnEXIV. She has been the leader of 20 projects and has participated in over 50 (10 for European Space Agency). She is author of 50 journal papers (20 related with Satcom) and more than 200 conference papers (20 invited). She is co-author of 4 books and 5 patents (1 on satcom). She has been guest editor in 5 special issues and currently she is editor of IEEE Transactions on Signal Processing and of Eurasip Signal Processing and Advances in Signal Processing. She has been the general chairman of IWCLD09, EUSIPCO11, EW14 and IWSCS14. She has participated in the organization of ESA conference 1996, SAM04 and she is the general chair of next ASMS16. She is the chair of next IEEE ICASSP20.